

## Proton-Neutron Mixed-Symmetry $3_{\text{ms}}^+$ State in $^{94}\text{Mo}$

N. Pietralla,\* C. Fransen, P. von Brentano, A. Dewald, A. Fitzler, C. Friebner, and J. Gableske

*Institut für Kernphysik, Universität zu Köln, D-50937 Köln, Germany*

(Received 26 August 1999)

We identify a  $J^\pi = 3_{\text{ms}}^+$  state in  $^{94}\text{Mo}$ . This identification is based on six  $M1$  and  $E2$  strengths and is the first identification of a  $3_{\text{ms}}^+$  state from  $B(M1)$  and  $B(E2)$  values. The transition strengths were determined from the measurement of Doppler shifts, branching ratios, and  $E2/M1$  mixing ratios, obtained from  $\gamma\gamma$  directional correlations following the  $^{91}\text{Zr}(\alpha, n)$  reaction and the  $\beta^+$  decay of  $^{94}\text{Tc}^m$ . The interacting boson model agrees with the observations, which prove the  $2^+$  mixed-symmetry states to be a building block in nuclear structure.

PACS numbers: 21.10.Re, 21.10.Tg, 23.20.Js, 27.60.+j

Atomic nuclei represent many-body quantum systems of strongly interacting fermions of two different species: protons and neutrons. Understanding of the proton-neutron (pn) symmetry of nuclear eigenstates is one of the fundamental aspects of nuclear structure physics. The nuclear shell model represents the theoretical tool to attack this problem. However, it suffers often from too large dimension. One way to radically truncate the shell model problem was suggested in terms of the interacting boson model.

The pn version of the interacting boson model (IBM-2) predicted a new class of collective nuclear states [1–4]. These states, described systematically in [5], are low-lying collective valence shell excitations, which are not symmetric with respect to the pn degree of freedom. Multiphonon states built on an isovector quadrupole surface excitation were suggested for vibrational nuclei already in the sixties [6]. However, at that time these states were predicted at a much higher energy. pn nonsymmetric states act in the IBM frame as building blocks of collective nuclear structure able to form multiphonon states. According to the algebraical approach, the pn symmetry of an IBM-2 wave function is quantified by the  $F$ -spin quantum number [1–3].  $F$ -spin is the isospin for the elementary proton and neutron bosons. IBM-2 wave functions with  $F$ -spin quantum numbers  $F < F_{\text{max}}$  contain at least one pair of proton and neutron bosons, which is antisymmetric under exchange of nucleon labels. Such states are called mixed-symmetry (MS) states. It is of great interest to identify and study such collective states. Their properties and spreading widths provide benchmarks for microscopic calculations [7] and help to better understand the pn degree of freedom in heavy nuclei. Information on two-phonon MS states is complementary to that from other multiphonon states as, e.g., isoscalar multiquadrupole phonon states or double-gamma excitations, since they involve another phonon: the MS quadrupole phonon.

Signatures of MS states, accessible to  $\gamma$  spectroscopy, are low excitation energy, weakly collective  $E2$  transitions to symmetric states, and strong  $M1$  transitions to symmetric states with matrix elements of about

$|\langle J_{\text{sym}}^f \parallel M1 \parallel J_{\text{ms}}^i \rangle| \approx 1 \mu_N$ . Two examples of MS states could already be identified from large  $M1$  strengths: the fundamental  $J^\pi = 2_{\text{ms}}^+$  state and the MS  $J^\pi = 1^+$  state. The  $1^+$  was the first MS state discovered experimentally [8,9]. The MS  $1^+$  state is called “scissors mode” due to its geometrical picture in rotors [10]. The  $2_{\text{ms}}^+$  state is the building block of MS structures in near-spherical nuclei. It can be excited from the ground state by a weakly collective  $E2$  transition with a few ( $\approx 0.2$ – $4$ ) single particle units, e.g., [11–13]. A coupling of the isoscalar quadrupole phonon to the  $2_{\text{ms}}^+$  state should lead to a  $(2_1^+ \otimes 2_{\text{ms}}^+)_{0^+,1^+,2^+,3^+,4^+}$  two-phonon multiplet [2,4–6] to which the MS  $1^+$  state belongs.

Other MS states were not identified from  $M1$  strengths. One-phonon  $2_{\text{ms}}^+$  states were observed [14] at low energies, where the level density is small and mixing may be weak. The MS  $1^+$  state could not mix with symmetric  $1^+$  configurations because the latter are absent in the IBM framework. It was still unknown whether MS multiphonon structures with  $J \neq 1$  exist. A clear identification of MS states with  $J \neq 1, 2$  based on  $M1$  strengths is necessary to enable the investigation of MS multiphonon structures. In some cases  $E2/M1$  mixing ratios were used to tentatively assign MS character to nuclear states with  $J > 2$ , e.g., [15,16]. However, the  $M1$  strengths were not measured, rendering the MS assignments uncertain. Besides the known one-phonon  $2_{\text{ms}}^+$  state and the two-phonon  $1_{\text{sc}}^+$  state, the two-phonon  $3_{\text{ms}}^+$  state is the most fundamental MS state. In nuclei of the  $100 < A < 200$  mass region, the energy of the two-phonon  $1_{\text{sc}}^+$  state is close to 3 MeV [17]. An observation of the two-phonon  $3_{\text{ms}}^+$  state allows one to measure the energy splitting of the MS two-phonon multiplet.

This Letter reports on the identification of a  $3_{\text{ms}}^+$  state from  $M1$  strengths. We investigated the nucleus  $^{94}\text{Mo}$ , for which the most complete data on MS  $1_{\text{sc}}^+$  and  $2_{\text{ms}}^+$  states are known from a combination of photon scattering and  $\gamma\gamma$ -coincidence studies following  $\beta$  decay [18].

In order to populate medium-spin states well above the yrast line in  $^{94}\text{Mo}$ , we used—besides the  $\beta^+$  decay of the  $(2)^+$  low-spin isomer  $^{94}\text{Tc}^m$  [18]—the “complete”

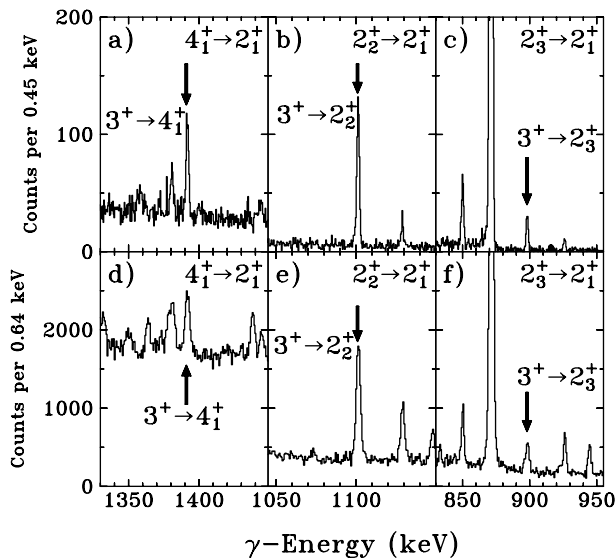


FIG. 1. Relevant parts of the  $\gamma\gamma$ -coincidence spectra from the  $\beta$  decay of  $^{94}\text{Tc}^m$  [(a)–(c)] and from the  $^{91}\text{Zr}(\alpha, n)$  reaction [(d)–(f)] gated with the 702.6 keV  $4_1^+ \rightarrow 2_1^+$  transition [(a),(d)], with the 993.2 keV  $2_2^+ \rightarrow 2_1^+$  transition [(b),(e)], and with the 1196.7 keV  $2_3^+ \rightarrow 2_1^+$  transition [(c),(f)]. The arrows mark the decays of the  $3^+$  state at 2965.4(2) keV.

cold ( $\alpha, n$ ) fusion reaction on  $^{91}\text{Zr}$  at the Coulomb barrier. A 15 MeV  $^4\text{He}$  beam was supplied by the Cologne FN Tandem Van De Graaff accelerator. A beam current of about 3 pA was used on a 11 mg/cm<sup>2</sup> zirconium target, enriched in  $^{91}\text{Zr}$  to 64%, on a 60 mg/cm<sup>2</sup> thick bismuth backing. The spin and parity quantum numbers  $J^\pi = 5/2^+$  of the  $^{91}\text{Zr}$  target nuclei favored the population of  $3^+$  states in the ( $\alpha, n$ ) reaction. The  $^{91}\text{Zr}(\alpha_{15\text{ MeV}}, n)^{94}\text{Mo}$  reaction leads to a maximum excitation energy of  $E_x^{\text{max}} = 9.2$  MeV for  $^{94}\text{Mo}$  and a grazing angular momentum of  $L_{\text{graz}} = 4\hbar$ . We used the OSIRIS spectrometer equipped with ten HPGe  $\gamma$  detectors. Six detectors were mounted perpendicular to the beam axis, two detectors were positioned at 45° and two at 135° with respect to the beam.  $\gamma$ -singles spectra and

$\gamma\gamma$ -coincidence events were recorded. Figure 1 shows  $\gamma\gamma$ -coincidence spectra observed in the  $^{91}\text{Zr}(\alpha, n)$  reaction and in the  $\beta$  decay of  $^{94}\text{Tc}^m$ . These spectra show three out of four observed  $\gamma$  transitions, which depopulate a  $3^+$  state at 2965.4 keV (the  $3^+ \rightarrow 2_1^+$  transitions are visible in the less clean  $2_1^+ \rightarrow 0_1^+$  coincidence spectra and are omitted in Fig. 1). These  $\gamma$  lines were observed in both experiments with almost equal relative intensities showing that the  $3^+$  state is no doublet. The measured properties of the four transitions are shown in Table I. Below we assign MS character to the  $3^+$  state at 2965.4(2) keV.

We first discuss the spin-parity assignment  $J^\pi = 3^+$ . Because of fast  $\gamma$  transitions to states with spin and parity  $J^\pi = 2^+, 4^+$ , the level at 2965.4 keV must have spin and parity quantum numbers  $2^+, 3^+, 4^+$ , or  $3^-$ , if we consider only  $M1, E2$ , or  $E1$  multipolarities.  $J^\pi = 3^+$  is favored by the measurement of the  $\log ft = 7.28(16)$  value [19,20] in the  $\beta$  decay of the  $(2)^+$  low-spin isomer  $^{94}\text{Tc}^m$  ruling out  $J^\pi = 4^+$ . The measured  $l = 0$  transfer [21] to the level at 2.966 MeV in the  $^{95}\text{Mo}(d, t)^{94}\text{Mo}$  neutron pickup reaction leaves the spin and parity assignments  $J^\pi = 2^+, 3^+$  as the only possibilities, while  $J^\pi = 3^+$  is favored [21]. (The energies of levels around 2.9 MeV are systematically overestimated in Ref. [21] by about 6 keV with respect to high-resolution  $\gamma$  spectroscopy. Since the level at 2.972 MeV from Ref. [21] is the only level with  $J < 4$  ever observed at this energy, we can identify it with the level at 2965.4 keV.) We use the  $\gamma\gamma$  angular correlations to assign  $J^\pi = 3^+$ . Figure 2 shows the deciding angular correlations. The hypothesis  $J^\pi = 2^+$  for the 2965.4 keV level cannot account for the observations for any  $M3/E2$  mixing ratio of the  $4_1^+ \rightarrow 2_1^+$  transition while the alternative hypothesis  $J^\pi = 3^+$  with a pure  $4_1^+ \rightarrow 2_1^+$   $E2$  transition describes the data well. The best agreement is obtained for a small  $E2/M1$  multipole mixing ratio  $\delta = -0.08(6)$  for the  $3^+ \rightarrow 4_1^+$  transition used in Fig. 2. The  $3^+ \rightarrow 4_1^+, 2_2^+$  transitions are approximately pure  $M1$  transitions (see Table I) and the  $3^+ \rightarrow 2_1^+, 2_3^+$  transitions have considerable  $E2$  admixtures.

TABLE I.  $\gamma$  decays of the  $3^+$  state at 2965.4 keV. Shown are the final states, the transition energies, and relative  $\gamma$  intensities from the  $\gamma\gamma$ -coincidence studies following the  $\beta$  decay of  $^{94}\text{Tc}^m$  and from the  $^{91}\text{Zr}(\alpha, n)$  reaction and the adopted  $E2/M1$  multipole mixing ratios from both measurements. Besides the unique  $\gamma\gamma$ -coincidence relations, the equality of the  $\gamma$  intensities from the two different reactions prove that the four  $\gamma$  transitions stem from the same level.

$J_f^\pi$	$E_\gamma$ (keV)		$I_\gamma$ (%)		$\delta$
	$\beta$ decay	$(\alpha, n)$	$\beta$ decay	$(\alpha, n)$	
$2_1^+$	2094.25(10)	2093.5(10)	36.9(14)	32(6)	$0.5^{+0.5}_{-0.3}$
$4_1^+$	1391.58(10)	1391.2(3)	63.0(24)	59(12)	-0.08(6)
$2_2^+$	1101.08(10)	1101.0(3)	100.0(23)	100(8)	-0.09(6)
$2_3^+$	898.10(10)	897.8(5)	23.0(12)	25(5)	$\left\{ \begin{array}{l} 0.39(25)^a \\ 2.0^{+1.2}_{-0.6} \end{array} \right.$
$0_1^+$	2965.3(2)		<0.5		

<sup>a</sup>The data agree with both mixing ratios.

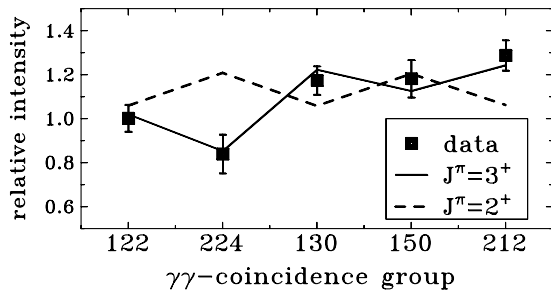


FIG. 2. Measurement of the spin quantum number  $J = 3$  for the level at 2965.4 keV. The solid squares show the measured relative intensities of the 703–1391 keV  $\gamma\gamma$  coincidence from the  $J_{2965}^{\pi} \text{ keV} \rightarrow 4_1^+ \rightarrow 2_1^+$   $\gamma\gamma$  cascade for five geometrically independent coincidence groups of our spectrometer. The coincidence groups are labeled by three integers, which denote in units of  $\pi/4$  the two angles between the observational directions and the beam and between the planes defined by the beam and by the  $\gamma$  directions. The lines represent the least-squares fits for the spin hypotheses  $J = 3$  and  $J = 2$ . The Gaussian width  $\sigma$  of the  $m$ -substate distribution and the  $J_{2965}^{\pi} \text{ keV} \rightarrow 4_1^+$  multipole mixing ratio  $\delta$  were treated as free parameters.

We extracted the lifetime of the  $3^+$  state from the line shapes of the  $3_{2965}^+ \rightarrow 2_2^+$  and  $3_{2965}^+ \rightarrow 4_1^+$  transitions. Figure 3 shows the 1101 keV line from the decay of the  $3_{2965}^+$  state to the  $2_2^+$  state observed under forward and backward angles and perpendicular to the beam axis in coincidence with the  $2_2^+ \rightarrow 2_1^+$  transition. The  $\gamma$  transitions depopulating the  $3_{2965}^+$  state are almost completely Doppler shifted. The mean recoil velocity of the  $^{94}\text{Mo}$  nuclei is  $v = 0.38\% c$ . The average stopping time in the  $^{91}\text{Zr}$  target is about 700 fs. We use the parameters [22]

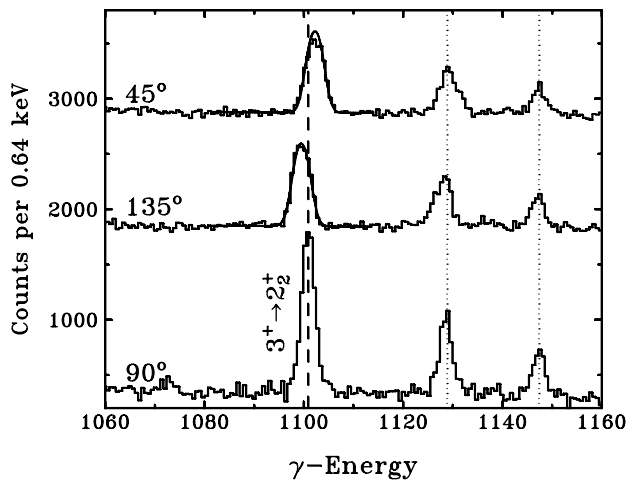


FIG. 3. Doppler shift of the 1101 keV  $3_{2965}^+ \rightarrow 2_2^+$  transition observed in coincidence with the (unshifted) 993 keV  $2_2^+ \rightarrow 2_1^+$  transition at the angles of  $45^\circ$  and  $135^\circ$  compared to the unshifted transition measured at  $90^\circ$ . The upper spectra are vertically displaced by 1800 counts ( $135^\circ$ ) and 2800 counts ( $45^\circ$ ). The dashed line marks the unshifted peak position. The curves show calculated line shapes using the observed 5% long-lived discrete feeding, 95% sidefeeding with a finite sidefeeding time  $\tau_{\text{SF}} = 80$  fs, and a level lifetime  $\tau(3^+) = 80$  fs.

$f_n = 0.7$  for the nuclear stopping and  $f_e = 1.03(0.81)$  and  $a = 0.579(0.611)$  for the electronic stopping in  $^{91}\text{Zr}$  ( $^{209}\text{Bi}$ ), where  $f_e, a$  were fitted to the semiempirical stopping powers from Ref. [23] with slight modifications as described in detail in Ref. [22]. The line shape analysis of the  $3_{2965}^+ \rightarrow 2_2^+, 4_1^+$  transitions yields a short effective lifetime  $\tau_{\text{eff}} = 200(30)$  fs. This effective lifetime is obtained consistently from the Doppler shifts of both the 1101 keV and the 1391 keV transitions. The effective lifetime represents an upper limit for the lifetime of the  $3^+$  state, while  $\tau(3^+)$  and  $\tau_{\text{eff}}$  would coincide in the limit of prompt sidefeeding. The measured Doppler shifts of the 1196.7 keV  $2_3^+ \rightarrow 2_1^+$  transition show that the assumption of a prompt sidefeeding cannot hold. The short lifetime  $\tau(2_3^+) = 60(9)$  fs of the  $2_3^+$  state was independently measured in a recent photon scattering experiment [18]. From its known lifetime we can estimate a sidefeeding time of  $\tau_{\text{SF}} = 80(20)$  fs for the  $2_3^+$  state in the present reaction by considering the observed 20% long-lived feeding through discrete transitions and an 80% sidefeeding with the time constant  $\tau_{\text{SF}}$ . In the line shape analysis for the  $3^+$  state, we used the conservative assumption of an equal sidefeeding time of  $\tau_{\text{SF}} = 80(20)$  fs for the  $2_3^+$  state and for the  $3_{2965}^+$  state. The measured line shapes are consistent with the  $3^+$  lifetime:

$$\tau(3_{2965}^+) = 80(30) \text{ fs}. \quad (1)$$

Calculated line shapes are shown in Fig. 3. The error quoted in Eq. (1) represents the statistical error. Not considered here is the uncertainty in the stopping power of 20%, which affects all  $M1$  and  $E2$  transitions from the  $3_{\text{ms}}^+$  state by the same factor and is not given in Tables II and III, because relative values are not affected.

Using this lifetime, the branching ratios, and the  $E2/M1$  mixing ratios, we obtain the transition strengths, which are listed in Table II. Indeed, the  $M1$  matrix elements of the  $3^+ \rightarrow 4_1^+, 2_2^+$  transitions are of the order

TABLE II. Measured decay transition strengths of the  $3^+$  state of  $^{94}\text{Mo}$  at 2965.4(2) keV excitation energy.

Observable	Unit	Expt.
$B(M1; 3_{\text{ms}}^+ \rightarrow 2_1^+)$	$(\mu_N^2)$	$0.010^{+0.012}_{-0.006}$
$B(M1; 3_{\text{ms}}^+ \rightarrow 4_1^+)$	$(\mu_N^2)$	$0.074^{+0.044}_{-0.019}$
$B(M1; 3_{\text{ms}}^+ \rightarrow 2_2^+)$	$(\mu_N^2)$	$0.24^{+0.14}_{-0.07}$
$B(M1; 3_{\text{ms}}^+ \rightarrow 2_{3,\text{ms}}^+)$	$(\mu_N^2)$	$\left\{ \begin{array}{l} 0.09^{+0.07}_{-0.03} \\ 0.021^{+0.035}_{-0.014} \end{array} \right.^a$
$B(E2; 3_{\text{ms}}^+ \rightarrow 2_1^+)$	(W.u.)	$0.4^{+1.0}_{-0.36}$
$B(E2; 3_{\text{ms}}^+ \rightarrow 4_1^+)$	(W.u.)	$<0.7$
$B(E2; 3_{\text{ms}}^+ \rightarrow 2_2^+)$	(W.u.)	$<4.0$
$B(E2; 3_{\text{ms}}^+ \rightarrow 2_{3,\text{ms}}^+)$	(W.u.)	$\left\{ \begin{array}{l} 10^{+12} \\ 8 \\ 60^{+47}_{-22} \end{array} \right.^a$
$B(M3; 3_{\text{ms}}^+ \rightarrow 0_1^+)$	$(\mu_N^2 b^2)$	$<330$

<sup>a</sup>For  $E2/M1$  mixing ratio  $\delta(3^+ \rightarrow 2_3^+) = 0.39(25)$  (top) and  $\delta(3^+ \rightarrow 2_3^+) = 2.0^{+1.2}_{-0.6}$  (bottom).

TABLE III. Comparison of analytical IBM-2 predictions for  $M1$  strengths (in  $\mu_N^2$ ) of MS states with data on  $^{94}\text{Mo}$  ( $1^+, 2^+$  data from Ref. [18]). Orbital values,  $g_\pi = 1 \mu_N$  and  $g_\nu = 0 \mu_N$ , are used for the boson  $g$  factors. Two different “cores” were assumed:  $^{90}\text{Zr}$  with proton boson number  $N_\pi = 1$  and  $^{100}\text{Sn}$  with  $N_\pi = 4$ .

IBM core	$^{90}\text{Zr}$		$^{100}\text{Sn}$		Expt.
	U(5)	O(6)	U(5)	O(6)	
Observable					
$B(M1; 1_{\text{ms}}^+ \rightarrow 0_1^+)$	0	0.08	0	0.16	0.16(1)
$B(M1; 1_{\text{ms}}^+ \rightarrow 2_2^+)$	0.84	0.84	0.33	0.36	0.43(5)
$B(M1; 2_{\text{ms}}^+ \rightarrow 2_1^+)$	0.36	0.36	0.23	0.30	0.48(6)
$B(M1; 3_{\text{ms}}^+ \rightarrow 2_2^+)$	0.41	0.41	0.16	0.18	$0.24^{+0.14}_{-0.07}$
$B(M1; 3_{\text{ms}}^+ \rightarrow 4_1^+)$	0.31	0.31	0.12	0.13	$0.074^{+0.044}_{-0.019}$

of one nuclear magneton:  $|\langle 4_1^+ || M1 || 3_{2965 \text{ keV}}^+ \rangle| = 0.72^{+0.19}_{-0.10} \mu_N$  and  $|\langle 2_2^+ || M1 || 3_{2965 \text{ keV}}^+ \rangle| = 1.30^{+0.33}_{-0.21} \mu_N$ . The  $E2$  transition to the  $2_1^+$  state may be weakly collective with a strength of about one Weisskopf unit. The  $3_{2965 \text{ keV}}^+ \rightarrow 2_3^+$  transition is consistent with a collective  $E2$  strength with tens of Weisskopf units. The uncertainties of the mixing ratios in both cases prevent definite numbers. As can be seen from Fig. 4, all decays are consistent with a MS two-phonon interpretation of the  $3^+$  state at 2965 keV, to which we, therefore, assign MS character. Table III compares the measured enhanced  $B(M1)$  values for MS states of  $^{94}\text{Mo}$  with the analytical predictions of the IBM-2. The IBM-2 predictions [5,24] for the  $3_{\text{ms}}^+$  state agree reasonably with the observations for the  $3^+$  state of  $^{94}\text{Mo}$  at 2965.4 keV. The qualitative MS assignment is obtained for both reasonable assumptions for the IBM core:  $^{90}\text{Zr}$  or  $^{100}\text{Sn}$ . Moreover, the data on the  $3_{\text{ms}}^+$  state are consistent with those on the previously identified  $1^+$  and  $2^+$  MS states of  $^{94}\text{Mo}$ .

In conclusion, the decay transition strengths of the  $3^+$  state of  $^{94}\text{Mo}$  at 2965.4 keV were measured, and we pro-

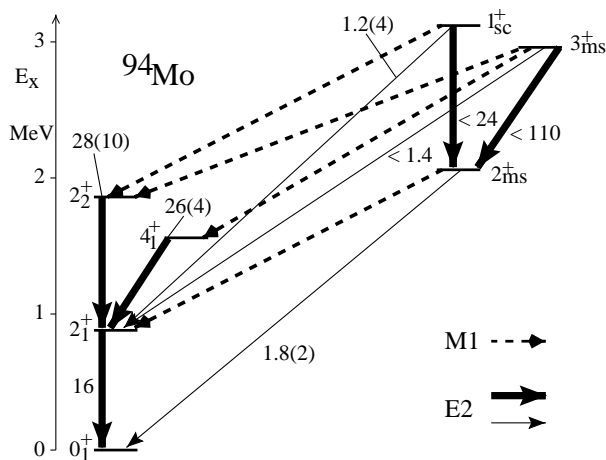


FIG. 4. Partial level scheme of  $^{94}\text{Mo}$ . The numbers denote measured  $B(E2)$  values in Weisskopf units (see Ref. [18]). For  $B(M1)$  values, see Table III.

pose this state as a realization of the  $3_{\text{ms}}^+$  state predicted by the IBM.

We thank S. Kasemann and I. Schneider for help and A. Gelberg, F. Iachello, R. V. Jolos, U. Kneissl, A. Leviatan, A. Lisetskiy, T. Otsuka, H. H. Pitz, A. Richter, I. Wiedenhöver, and A. Zilges for discussions. Supported by the DFG under Grants No. Br 799/9-1 and No. Pi 393/1-1.

\*Present address: Wright Nuclear Structure Laboratory, Yale University, New Haven, CT 06520.

- [1] A. Arima, T. Otsuka, F. Iachello, and I. Talmi, Phys. Lett. **66B**, 205 (1977).
- [2] T. Otsuka, Ph.D. thesis, University of Tokyo, 1978 (unpublished).
- [3] T. Otsuka, A. Arima, and F. Iachello, Nucl. Phys. **A309**, 1 (1978).
- [4] F. Iachello, Phys. Rev. Lett. **53**, 1427 (1984).
- [5] P. Van Isacker, K. Heyde, J. Jolie, and A. Sevrin, Ann. Phys. (N.Y.) **171**, 253 (1986).
- [6] Amand Faessler, Nucl. Phys. **85**, 653 (1966).
- [7] L. Zamick, Phys. Rev. C **31**, 1955 (1985).
- [8] D. Bohle, A. Richter, W. Steffen, A.E.L. Dieperink, N. Lo Iudice, F. Palumbo, and O. Scholten, Phys. Lett. **137B**, 27 (1984).
- [9] A. Richter, Prog. Part. Nucl. Phys. **34**, 261 (1995).
- [10] N. LoIudice and F. Palumbo, Phys. Rev. Lett. **41**, 1532 (1978).
- [11] W.J. Vermeer, C.S. Lim, and R.H. Spear, Phys. Rev. C **38**, 2982 (1988).
- [12] B. Fazekas, T. Belgya, G. Molnár, A. Veres, R. A. Gatenby, S. W. Yates, and T. Otsuka, Nucl. Phys. **A548**, 249 (1992).
- [13] N. Pietralla *et al.*, Phys. Rev. C **58**, 796 (1998).
- [14] W.D. Hamilton, A. Irbäck, and J.P. Elliott, Phys. Rev. Lett. **53**, 2469 (1984).
- [15] S.T. Ahmad, W.D. Hamilton, P. Van Isacker, S.A. Hamada, and S.J. Robinson, J. Phys. (London) **G15**, 93 (1989).
- [16] A. Giannatiempo, A. Nannini, and P. Sona, Phys. Rev. C **58**, 3316 (1998); **58**, 3335 (1998).
- [17] N. Pietralla, P. von Brentano, R.-D. Herzberg, U. Kneissl, N. Lo Iudice, H. Maser, H.H. Pitz, and A. Zilges, Phys. Rev. C **58**, 184 (1998).
- [18] N. Pietralla, C. Fransen, D. Belic, P. von Brentano, C. Frießner, U. Kneissl, A. Linnemann, A. Nord, H.H. Pitz, T. Otsuka, I. Schneider, V. Werner, and I. Wiedenhöver, Phys. Rev. Lett. **83**, 1303 (1999).
- [19] J.K. Tuli, Nucl. Data Sheets **66**, 1 (1992).
- [20] J. Barrette, A. Boutard, and S. Monaro, Can. J. Phys. **47**, 995 (1969).
- [21] J.E. Holden and W.W. Daehnick, Phys. Rev. C **8**, 2286 (1973).
- [22] P. Petkov *et al.*, Nucl. Phys. **A640**, 293 (1998).
- [23] L.C. Northcliffe and R.F. Schilling, Nucl. Data Tables **A7**, 233 (1970).
- [24] C. De Coster, K. Heyde, S. Rombouts, and A. Richter, Phys. Rev. C **51**, 3510 (1995).